Published in final edited form as:
Science. 2004 June 4; 304(5676): 1509–1513.

Mutations in a Human *ROBO* Gene Disrupt Hindbrain Axon Pathway Crossing and Morphogenesis

Joanna C. Jen[1,*], **Wai-Man Chan**[7], **Thomas M. Bosley**[10], **Jijun Wan**[1], **Janai R. Carr**[1], **Udo Rüb**[11], **David Shattuck**[1], **Georges Salamon**[2], **Lili C. Kudo**[3], **Jing Ou**[1], **Doris D. M. Lin**[12], **Mustafa A. M. Salih**[13], **Tülay Kansu**[14], **Hesham al Dhalaan**[15], **Zayed al Zayed**[16], **David B. MacDonald**[15], **Bent Stigsby**[15], **Andreas Plaitakis**[17], **Emmanuel K. Dretakis**[18], **Irene Gottlob**[19], **Christina Pieh**[20], **Elias I. Traboulsi**[21], **Qing Wang**[21], **Lejin Wang**[21,†], **Caroline Andrews**[7,9], **Koki Yamada**[7,9], **Joseph L. Demer**[1,4], **Shaheen Karim**[4], **Jeffry R. Alger**[2], **Daniel H. Geschwind**[1], **Thomas Deller**[11], **Nancy L. Sicotte**[1], **Stanley F. Nelson**[5], **Robert W. Baloh**[1,6], and **Elizabeth C. Engle**[7,8,9,*]

1 *Department of Neurology,*

2 *Department of Radiology,*

3 *Interdepartmental Program in Neurosciences,*

4 *Department of Ophthalmology,*

5 *Department of Human Genetics,*

6 *Department of Surgery, University of California, Los Angeles, CA 90095, USA.*

7 *Division of Genetics,*

8 *Department of Neurology, Children's Hospital Boston, and*

9 *Harvard Medical School, Boston, MA 02115, USA.*

10 *Neuro-ophthalmology Division, King Khaled Eye Specialist Hospital, Riyadh, Saudi Arabia.*

11 *Institute of Clinical Neuroanatomy, J. W. Goethe University, 60590 Frankfurt/M, Germany.*

12 *Department of Radiology and Radiologic Science, Johns Hopkins University School of Medicine, Baltimore, MD 21287, USA.*

13 *Department of Pediatrics, King Khalid University Hospital, Riyadh, Saudi Arabia.*

14 *Neuro-Ophthalmology Unit, Hacettepe University Hospitals, Ankara, Turkey.*

15 *Neuroscience Department,*

16 *Surgery Department, King Faisal Specialist Hospital and Research Centre, Riyadh, Saudi Arabia.*

17 *Department of Neurology,*

18 *Department of Orthopaedics-Traumatology, University of Crete, Heraklion, Crete, Greece.*

*To whom correspondence should be addressed. E-mail: jjen@ucla.edu (J.C.J.); engle@enders.tch.harvard.edu (E.C.E.)
†Present address: Laboratory of Molecular Ophthalmic Genetics, Department of Pediatric Ophthalmology and Strabismus, Peking University Eye Center, Peking University No. 3 Hospital.

Supporting Online Material
www.sciencemag.org/cgi/content/full/1096437/DC1
Patients and Methods
Figs. S1 and S2
Tables S1 to S3
References

19 *Department of Ophthalmology, Leicester University, Leicester, UK.*

20 *University Eye Clinic, University of Freiburg, Freiburg, Germany.*

21 *Cleveland Clinic Foundation, Cleveland, OH, USA.*

Abstract

The mechanisms controlling axon guidance are of fundamental importance in understanding brain development. Growing corticospinal and somatosensory axons cross the midline in the medulla to reach their targets and thus form the basis of contralateral motor control and sensory input. The motor and sensory projections appeared uncrossed in patients with horizontal gaze palsy with progressive scoliosis (HGPPS). In patients affected with HGPPS, we identified mutations in the *ROBO3* gene, which shares homology with *roundabout* genes important in axon guidance in developing *Drosophila*, zebrafish, and mouse. Like its murine homolog Rig1/Robo3, but unlike other Robo proteins, ROBO3 is required for hindbrain axon midline crossing.

Molecular mechanisms guide neuronal cell bodies and their axons toward their final destination, thereby generating brain structures as the advancing growth cones are attracted or repelled by guidance molecules. Ipsilaterally projecting axons must resist crossing the midline of the central nervous system, whereas contralaterally projecting axons must cross once and only once. Axon guidance molecules include the roundabout (robo) family of transmembrane receptors, identified in *Drosophila* mutants in which axons cross and recross the midline (*1*). Robo proteins activated by chemorepellent Slit prevent axons from inappropriately crossing the midline (*2*–*4*), specify the lateral position of longitudinal pathways (*5*), and direct cell migration (*6*). Robo proteins interact with other signaling molecules to modify cytoskeletal assembly and regulate turning of a growing axon (*7*).

The syndrome of horizontal gaze palsy with progressive scoliosis [HGPPS; Online Mendelian Inheritance in Man (OMIM) 607313] with hindbrain dysplasia is a rare human disorder (*8*, *9*). Studies of human genetic disorders affecting eye movement helped define neuronal codes that underlie axon pathfinding (*10*–*12*). HGPPS is characterized by absence of conjugate horizontal eye movement and scoliosis that often requires surgical intervention early in life (Fig. 1) (*13*, *14*). Horizontal gaze palsy may be due to defects in the abducens nuclei (CN VI), which contain both ipsilaterally projecting motor neurons and contralaterally projecting interneurons, or supranuclear control regions such as the pontine paramedian reticular formation (PPRF) that projects to the abducens and oculomotor nuclei (*15*).

HGPPS is autosomal recessive, and the HG-PPS disease locus in two consanguineous families (fig. S1) is within a 30-centimorgan region on chromosome 11q23–25 (*8*). We have now identified eight additional consanguineous HG-PPS families (fig. S1 and Table 1). Their HGPPS phenotypes are consistent with linkage to the 11q23–25 locus, and affected individuals are homozygous in the candidate region.

To further characterize the functional neuroanatomical defects, we performed neuroimaging and functional evoked-potential studies in these HGPPS patients. Published neuroimaging results have been normal in some but not all cases of HGPPS (*9*, *15*, *16*). We carried out high-resolution magnetic resonance (MR) imaging studies in eight patients from four families (pedigrees 1, 2, 4, AX; Table 1; fig. S1). Abnormal flattening of the basis pontis and hypoplasia in the pontine tegmentum were evident on sagittal sections (Fig. 2, A and D). The structural alterations in caudal pons suggested potential involvement of the abducens nuclei, the medial longitudinal fasciculus, and the PPRF (Fig. 2, B and E, and fig. S2). The medulla appeared abnormally butterfly-like, with anterior flattening and an unusual midline cleft (Fig. 2, C and F). The abducens nerves were visualized bilaterally in the extra-axial space (*17*, *18*), and orbital

MRI demonstrated normal extraocular muscle configuration and size, as well as the presence of apparently normal intraorbital motor nerves to the medial and lateral rectus muscles (*18*). Therefore, the absence of bulging of abducens nuclei into the IVth ventricle observed in HGPPS patients likely represents hypoplasia rather than absence of the abducens nuclei. These findings distinguish HGPPS from other congenital eye movement disorders in which absent or aberrant motor nerves are associated with hypoplastic extraocular muscles but normal brain structure (*10–12*).

To investigate physiology of the major axon pathways, we conducted evoked-potential studies (Fig. 2, G and H). The longest projecting axon pathway in the mammalian central nervous system, the corticospinal tract, originates in the motor cortex, crosses the midline in the medulla, fasciculates, and descends to synapse on α–motor neurons throughout the spinal cord. Decussation of the corticospinal tract in the medulla is the anatomical basis for voluntary motor control by the contralateral motor cortex. Sensory axons conveying discriminative touch, vibration, and proprioception ascend in the dorsal columns of the spinal cord, decussate as internal arcuate fibers in the medulla, then project via the medial lemniscus to the thalamus. Decussation of these sensory fibers in the medulla forms the anatomical basis for sensory input to the contralateral sensory cortex (*19*). Spinothalamic pathways for pain and temperature, however, decussate in the cord and are not assessed by normal somatosensory evoked-potential studies.

In normal subjects, contralateral sensorimotor projection is the rule (Fig. 2G) (*20*). Somatosensory evoked potential studies in all four HG-PPS patients available for study (from pedigrees 1, 2, 4; Table 1, fig. S1, and Fig. 2H) showed abnormally reversed lateralization of these responses, indicating uncrossed ascending dorsal column-medial lemniscal sensory pathways. Similarly, motor evoked-potential studies in these patients demonstrated abnormally ipsilateral muscle responses, reflecting uncrossed descending corticospinal motor pathways. Uncrossed corticospinal and dorsal column-medial lemniscal pathways and the abnormal midline cleft in the medulla observed in these patients suggest the absence of pyramidal and internal arcuate decussations and a role for the HGPPS gene in hindbrain axon pathway crossing and morphogenesis.

To identify the HGPPS gene, we used closely spaced microsatellite markers on 11q23–25. Linkage analysis of two of the pedigrees revealed recombination events in affected individuals that reduced the HGPPS region to 2.4 Mb flanked by microsatellite markers D11S4464 and D11S990 (fig. S1). Annotated genes in the candidate region showed no pathogenic variants (Fig. 3A). However, one predicted 4-kb mRNA, NT_033899.598, was promising because it shares homology with *Rig1* in mouse (*21*) and *robo3* in zebrafish (*22*), both of which are members of the *roundabout* gene family (Fig. 3B). The 3′ end of NT_033899.598 overlaps with the 1779–base pair (bp) human *RBIG1* gene, the product of which shares homology with the cytoplasmic domain of mouse Rig1. Indeed, we identified mutations to establish that this is the HGPPS gene and named it *ROBO3* (Table 1). The gene is expressed in fetal human brain (Fig. 3E).

The predicted genomic structure of human *ROBO3* was refined by reverse transcription polymerase chain reaction (RT-PCR) of fetal human brain polyadenylated RNA. There appear to be multiple alternative splice forms of *ROBO3*, with the longest deduced open reading frame consisting of 28 exons, spanning approximately 16,000 bases, and encoding a 1384–amino acid protein (Fig. 3C; GenBank AY509035). Homologous to other members of the roundabout family, the predicted amino acid sequence of ROBO3 contains a putative extracellular segment with five immunoglobulin (Ig)-like motifs and three fibronectin (Fn)-like motifs, a transmembrane segment, and an intracellular segment with three cytoplasmic signaling motifs: CC0, CC2, and CC3 (Fig. 3D). The CC1 motif, which is absent in human ROBO3 and mouse

Rig1 but present in other homologs, has been shown to interact with DCC to silence Netrin-1–attractive effects (*23*).

By sequencing all 28 exons and flanking introns in 10 HGPPS index patients, we identified 10 different homozygous mutations scattered throughout the *ROBO3* gene (Fig. 3D and Table 1). In the remaining members of each family, these mutations were homozygous in all affected but in no unaffected individuals and were heterozygous in obligate carriers. By pyro-sequencing, denaturing high-performance liquid chromatography, and/or restriction digest, the mutations were not found in ethnically mixed control individuals (n = 93 to 197) (Table 1).

We identified one nonsense, one splice site, and two frameshift mutations, all predicted to prematurely terminate the ROBO3 protein. In addition, we identified six missense mutations: four of which result in non-conservative changes in amino acid residues that are evolutionarily conserved. The affected amino acids (*24*) include L5, I66, G361, and R703, which are highly conserved across many species, and E319 and S705, which are conserved in human and mouse.

Nine of the 10 mutations are located in the extracellular domains of the ROBO3 protein (Fig. 3D). One nonsense (G456X) mutation and three missense mutations (I66L, E319K, G361E) are near or in the Ig-like domains. Two missense (R703P, S705P), one frameshift (insC), and one splice donor site (IVS13+1 G>A) mutation reside in the Fn-like domains. The missense mutations may alter ligand recognition, protein folding, or targeting. Missense mutation L5P is in the predicted signal sequence important for posttranslational membrane targeting and insertion. Although a proline for leucine substitution does not alter the net charge, it may disrupt the secondary structure of the signal sequence. Such a conservative amino acid change has indeed been shown to abolish the surface expression of other proteins (*25*).

The single intracellular mutation we identified, insG in exon 23, is predicted to incorporate novel sequences following CC2 and result in premature termination of the ROBO3 protein. If stable, the truncated receptor should retain much of the wild-type protein except for the C terminus where CC3 resides. Therefore, it is possible that CC3 is required for the normal function of ROBO3; alternatively, the frameshift mutation may interfere with protein folding and trafficking.

Different mutations throughout the predicted coding region for *ROBO3* leading to the same clinical manifestations provide evidence that *ROBO3* is the gene responsible for HGPPS. The requirement that mutations be present on both alleles of *ROBO3* for the manifestation of HGPPS to occur suggests that the mutations cause loss of gene function.

In situ hybridization demonstrated abundant expression of the *ROBO3* gene in the basis pontis in 15-week-old and 19-week-old fetal human brain (Fig. 3E). This observation is consistent with the hindbrain-specific expression of the homologous gene in mouse (*21*, *26*).

Our imaging and electrophysiological data suggest that ROBO3 differs from the other members of the roundabout family mediating repulsive axon guidance in that ROBO3 is required for crossing. Similarly, a role for the murine homolog, Rig1/Robo3, in promoting midline crossing has recently been demonstrated through genetic analysis (*27*). Notably, removal of mouse Rig1/Robo3 results in a complete failure of commissural axons to cross the midline throughout the spinal cord and the hindbrain. Thus, ROBO3 is required for midline crossing in both mouse and humans. In mouse, it was shown further that Rig1/Robo3 normally allows midline crossing by blocking axonal responses to repulsive midline Slit proteins; this is the opposite function of other Robo proteins, which mediate repulsive Slit signals and thus prevent mid-line crossing. The similarity of the phenotypes observed in humans and in mice with defects in *ROBO3* suggests that this divergent mechanism of action of ROBO3 is conserved across evolution.

The hindbrain abnormalities in HGPPS patients have not been completely characterized. The ascending sensory and descending motor pathways normally destined to cross the midline in the medulla failed to do so in HGPPS patients. Yet, neurologically, these patients are remarkably intact, with no apparent weakness, numbness, or incoordination. These findings suggest apparently normal sensorimotor integration and that the axon pathways responded appropriately to short-range and long-range cues to find their targets, albeit contralateral to the targets in normal subjects.

The major disability in this disorder arises from progressive scoliosis. It remains unknown whether the origin of scoliosis is musculoskeletal or neurogenic, but a neurogenic mechanism is possible in light of our structural data. Descending reticulospinal fiber tracts in the reticular formation, along with the corticospinal tract, mediate control signals from the brain to the spinal cord to drive locomotion and regulate muscle tone (*28*, *29*). Our imaging data indicate maldevelopment of these extrapyramidal projections in the reticular formation of HGPPS patients, which could, in turn, lead to progressive scoliosis.

The syndrome of HGPPS provides an exceptional opportunity for the functional characterization of a brain development gene *ROBO3* that defines a critical determinant in axon path finding and brain morphogenesis in human. ROBO3, along with its mouse homolog Rig1 (*27*), expands the role of the robo family of proteins previously known to prevent aberrant crossing.

References

1. Seeger M, Tear G, Ferres-Marco D, Goodman CS. Neuron 1993;10:409. [PubMed: 8461134]
2. Kidd T, et al. Cell 1998;92:205. [PubMed: 9458045]
3. Brose K, et al. Cell 1999;96:795. [PubMed: 10102268]
4. Fricke C, Lee JS, Geiger-Rudolph S, Bonhoeffer F, Chien CB. Science 2001;292:507. [PubMed: 11313496]
5. Rajagopalan S, Vivancos V, Nicolas E, Dickson BJ. Cell 2000;103:1033. [PubMed: 11163180]
6. Wu W, et al. Nature 1999;400:331. [PubMed: 10432110]
7. Patel BN, Van Vactor DL. Curr Opin Cell Biol 2002;14:221. [PubMed: 11891122]
8. Jen J, et al. Neurology 2002;59:432. [PubMed: 12177379]
9. Pieh C, Lengyel D, Neff A, Fretz C, Gottlob I. Neurology 2002;59:462. [PubMed: 12177390]
10. Nakano M, et al. Nature Genet 2001;29:315. [PubMed: 11600883]
11. Al-Baradie R, et al. Am J Hum Genet 2002;71:1195. [PubMed: 12395297]
12. Yamada K, et al. Nature Genet 2003;35:318. [PubMed: 14595441]published online 2 November 2003.
13. Dretakis EK, Kondoyannis PN. J Bone Joint Surg Am 1974;56:1747. [PubMed: 4434049]
14. Sharpe JA, Silversides JL, Blair RD. Neurology 1975;25:1035. [PubMed: 1237821]
15. Yee RD, Duffin RM, Baloh RW, Isenberg SJ. Arch Ophthalmol 1982;100:1449. [PubMed: 7115172]
16. Steffen H, Rauterberg-Ruland I, Breitbach N, Thomsen M, Kolling GH. Neuropediatrics 1998;29:220. [PubMed: 9762700]
17. T. M. Bosley, D. D. M. Lin, J. C. Jen, unpublished observations.
18. J. L. Demer, S. S. Karim, E. C. Engle, unpublished observations.
19. Parent, A. Carpenter's Human Neuroanatomy. ed. 9. Williams & Wilkins; Baltimore: 1996.
20. Lesser RP, et al. Neurology 1987;37:82. [PubMed: 3796841]
21. Yuan S, Cox L, Dasika G, Lee E. Dev Biol 1999;207:62. [PubMed: 10049565]
22. Lee JS, Ray R, Chien CB. Dev Dyn 2001;221:216. [PubMed: 11376489]
23. Stein E, Tessier-Lavigne M. Science 2001;291:1928. [PubMed: 11239147]

24. Single-letter abbreviations for the amino acid residues are as follows: A, Ala; C, Cys; D, Asp; E, Glu; F, Phe; G, Gly; H, His; I, Ile; K, Lys; L, Leu; M, Met; N, Asn; P, Pro; Q, Gln; R, Arg; S, Ser; T, Thr; V, Val; W, Trp; and Y, Tyr.

25. Lanza F, et al. Br J Haematol 2002;118:260. [PubMed: 12100158]

26. Camurri L, Mambetisaeva E, Sundaresan V. Gene Expr Patterns 2004;4:99. [PubMed: 14678835]

27. Sabatier C, et al. Cell 2004;117:157. [PubMed: 15084255]

28. Kuypers H. Prog Brain Res 1982;57:381. [PubMed: 6818612]

29. Kuypers, H. Brain Stem Control of Spinal Mechanisms. American Elsevier; New York: 1982. p. 29-54.

30. Supported by NIH DC05524 (R.W.B.); DC00162 and EY15311 (J.C.J.); MH60233 (D.H.G.); EY12498, EY13583, EY15298, and the Children's Hospital Mental Retardation Research Center P30 HD 18655 (E.C.E.); and UCLA Neurology (J.C.J.).

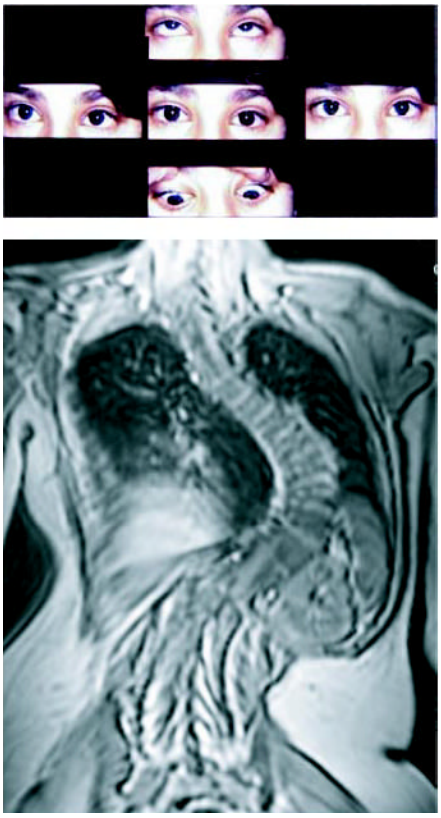

Fig 1.

HGPPS clinical profile. (**Top**) Photographs of an affected member with HGPPS demonstrating absent horizontal eye movement on attempted gaze to right (left) or left (right) but normal vertical gaze upward (upper) and downward (lower) from the primary position (central). (**Bottom**) A coronal scout MR imaging of the thoracic and lumbar spine demonstrating profound scoliosis.

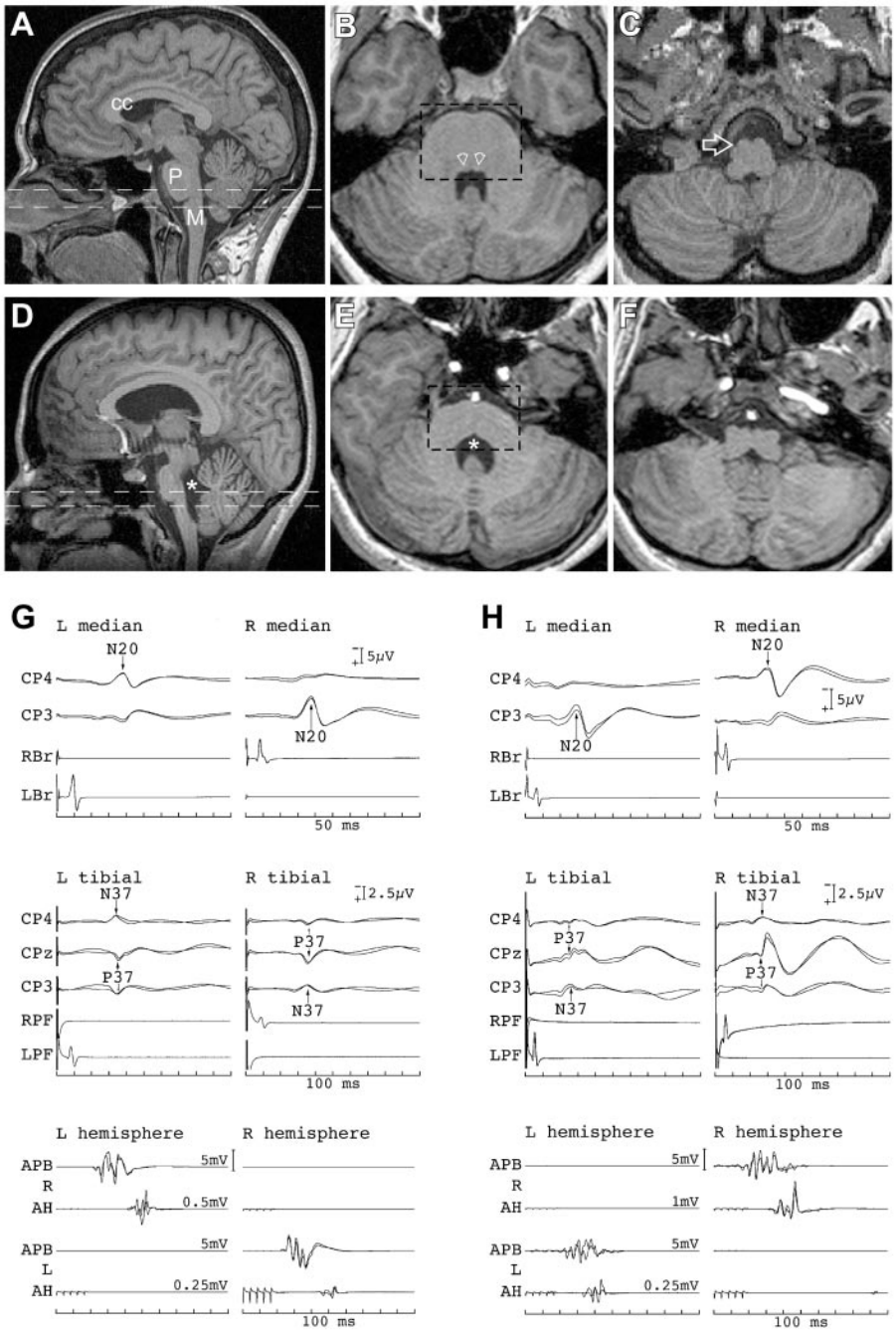

Fig 2.

Functional anatomical defects in HGPPS. Brain MR images of a normal subject (**A** to **C**) and an HGPPS patient (**D** to **F**) at comparable anatomical levels. (A and D) Sagittal view. Normal appearance of cortex and corpus callosum (cc) but dysmorphic hindbrain with enlarged fourth ventricle (*) in the patient. Dashed lines represent sections through pons (P) and medulla (M) shown in (B to F). (B and E) Axial view, caudal pons in box (see fig. S2 for details). Note hypoplasia, enlarged fourth ventricle, absent protrusions of the abducens nuclei (arrowheads) in the patient. (C and F) Axial view, medulla. Note flattened, butterfly-like appearance with deep midline cleft in the patient, compared with the rounded appearance in the control (open arrow). (**G** and **H**) Representative somatosensory and motor evoked-potential studies

demonstrating sensorimotor nondecussation in an HGPPS patient (H) compared with control (G). (Top) Bilateral peripheral nerve in the arms (Br, brachial-medial arm just above the antecubital fossa) and scalp recordings following left and then right median nerve stimulation. The N20 cortical sensory response was abnormally ipsilateral in patient. CP4, CPz, and CP3 are right, midline, and left centro-parietal scalp sites, respectively (mastoid reference). (Middle) Bilateral peripheral nerve in the legs (PF, popliteal fossa) and scalp recordings following left and then right tibial nerve stimulation. The cortical sensory response showed abnormally reversed P37/N37 lateralization in patient. (Bottom) Note abnormally ipsilateral hand (APB, abductor pollicis brevis) and foot (AH, abductor hallucis) muscle responses in patient compared with contralateral responses in control following transcranial electric stimulation of the left and then right hemisphere.

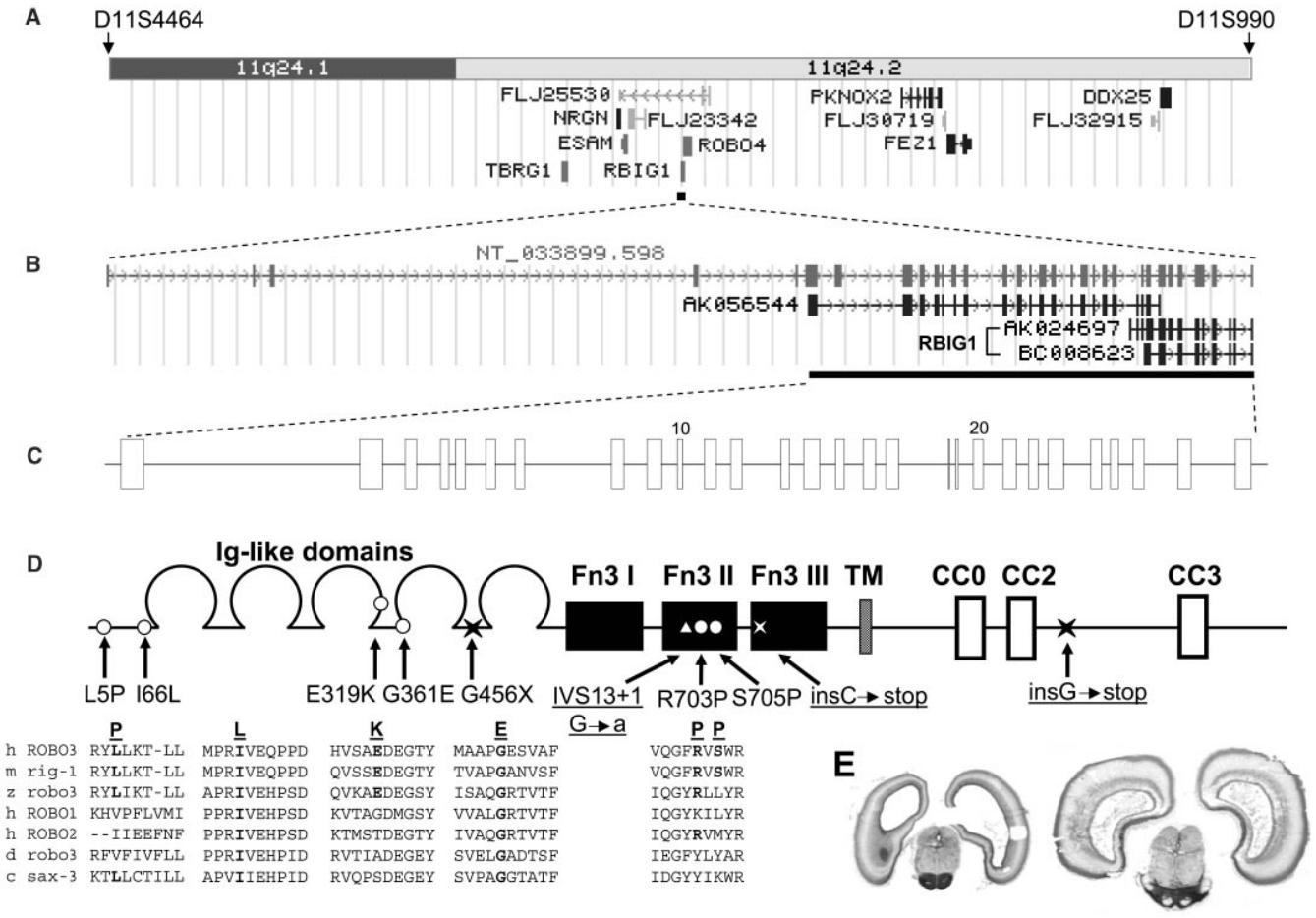

Fig 3.

(**A**) Physical map of the HGPPS region with annotated genes (UCSC Human Genome Browser July 2003 freeze) screened for mutations. (**B**) A GenScan-predicted hypothetical gene NT_033899.598 overlaps with AK056544 and BC008623 (also annotated as *RBIG1*). (**C**) Refinement of genomic structure of *ROBO3*; exons are represented by open boxes. (**D**) Predicted ROBO3 topology and locations of 10 homozygous mutations. The mutated residues are conserved, as demonstrated by aligning orthologous and paralogous sequences in human (h), mouse (m), zebrafish (z), *Drosophila* (d), and *C. elegans* (c). (**E**) In situ hybridization analysis of *ROBO3*, with intense signal from an antisense *ROBO3* probe in the basis pontis of fetal human brain at 15 weeks (left) and 19 weeks (right).

Table 1

Summary of patient ethnic origin and mutations.

Family	Ethnicity	Exon	Nucleotide change	Amino acid change	Domain	Controls screened
1	Indian	7	1082G>A	G361E	Ig IV	95
2	Saudi	23	3325 + 1 G	Frameshift	CC 2-3	116
3	Turkish	14	2108G>C	R703P	Fn3 II	150
4	Saudi	14	2113T>C	S705P	Fn3 II	116
5	Turkish	9	1366G>T	G456stop	Ig IV-V	95
GD	Greek	6	955G>A	E319K	Ig III	197
AX	Pakistani	15	2310 + 1 C	Frameshift	Fn3 III	106
JJ	Italian	1	14T>C	L5P	N-term	106
JF	Greek	2	196A>C	I66L	Ig I	175
JK	Arab	13	IVS13 + 1 G>A	Aberrant splicing	Fn3 II	93